Journal of Catalysis 268 (2009) 156–164

Contents lists available at ScienceDirect

Journal of Catalysis

journal homepage: www.elsevier.com/locate/jcat

Local environment of vanadium in V/Al/O-mixed oxide catalyst for propane ammoxidation: Characterization by *in situ* valence-to-core X-ray emission spectroscopy and X-ray absorption spectroscopy

O.V. Safonova [a], M. Florea [b], J. Bilde [c], P. Delichere [c], J.M.M. Millet [c,*]

[a] Swiss-Norwegian Beamlines (SNBL), European Synchrotron Radiation Facility, 6 rue Jules Horowitz, 38043 Grenoble Cedex, France
[b] University of Bucharest, Faculty of Chemistry, B-dul Regina Elisabeta 4-12, 030016 Bucharest, Romania
[c] Institut de Recherches sur la Catalyse et l'Environnement de Lyon, IRCELYON, UMR5256, CNRS-Université Claude Bernard Lyon 1, 2 Avenue A. Einstein, F-69626 Villeurbanne Cedex, France

ARTICLE INFO

Article history:
Received 26 May 2009
Revised 16 September 2009
Accepted 18 September 2009
Available online 21 October 2009

Keywords:
Acrylonitrile
Ammoxidation
Vanadium–aluminum oxynitride
Valence-to-core X-ray emission spectroscopy at V Kβ lines
V K-edge X-ray absorption spectroscopy
XPS

ABSTRACT

The local environment of vanadium in V/Al/O amorphous oxide catalyst has been studied under propane ammoxidation reaction conditions. *In situ* valence-to-core X-ray emission spectroscopy (XES) and X-ray absorption spectroscopy (XAS) at the V K-edge showed that acrylonitrile production starts when vanadium in the bulk structure of the oxide material changes its formal oxidation state from +4.8 to +3.8 ± 0.1. Exposure of the catalyst to pure NH_3 at 500 °C leads to further reduction of vanadium. Valence-to-core XES has also proved that the level of bulk nitridation of vanadium in the active catalyst was rather small. XPS analysis performed *ex situ* after the catalytic tests confirmed the presence of significant amounts of N^{3-}, NH_x, and –NN– species on the catalyst surface. It can be concluded that activation of V/Al/O catalyst on-stream is mainly associated with reduction of vanadium in the bulk structure of the material and nitridation of vanadium atoms on the surface.

1. Introduction

The substitution of alkenes by alkanes as a feedstock is a challenging task for industries producing chemicals, plastics, and synthetic fibers. It is also important for lowering the prices and risks of chemical storage, which become crucial due to the continuous increase of the worldwide demand for chemicals and the reinforcement of the legislation rules on their manipulation.

The challenge lies mainly in the difficulty of breaking the first C–H bond in alkane and the lack of stability of the products formed. The process of acrylonitrile (ACN) production from propane is one of the closest to be industrialized. In general nitriles are much more stable than the corresponding aldehydes or acids, which can also be produced from alkanes. Furthermore, the yield of nitriles can be high enough to sustain an industrial application. The known catalysts for propane ammoxidation into ACN are mainly based on either rutile-type metal antimonates (V/Sb/O, V/Al/Sb/O) [1–5] or mixed molybdates (Mo/V/Te(Sb)/Nb/O) [6–9]. Attempts to optimize these materials by tuning their composition were successful but not good enough for industrialization [10–12]. Recently discovered V/Al/O-mixed amorphous oxides catalysts have shown to be very promising for propane ammoxidation [13–18]. Moreover, it was demonstrated that catalytic performance of these oxides could be improved after their exposure on-stream under catalytic conditions or after preliminary annealing in NH_3 at high temperatures. These phenomena were explained by partial substitution of nitrogen for oxygen in the mixed oxide structure of the catalyst. Maximal concentration of nitrogen observed in this kind of material was 3–5 wt% [17]. The activity of V/Al/O catalysts was explained by a Mars–van Krevelen-type mechanism related to the lattice oxygen and nitrogen mobility as well as the redox activity of vanadium [17,18]. It was also demonstrated that catalytic performance of these materials strongly depends on various parameters such as: (i) the V/Al ratio, (ii) the pH during synthesis, (iii) the vanadium concentration in solution, and (iv) the nitridation protocol (temperature, nitridation mixture, and time) [16].

The V/Al/O catalytic system seems to be rather simple and has potential to be further improved. However, these materials have amorphous structure, which makes rather difficult understanding of relationships between their structure, composition, and catalytic properties. Recently, *in situ* XAS studies have shown that under reaction conditions of ACN production, vanadium in the bulk oxide structure changes its local coordination from tetrahedral (similar

* Corresponding author. Fax: +33 4 72 44 53 99
E-mail address: jean-marc.millet@ircelyon.univ-lyon1.fr (J.M.M. Millet).

0021-9517/$ - see front matter © 2009 Elsevier Inc. All rights reserved.
doi:10.1016/j.jcat.2009.09.014

to NH_4VO_3) to octahedral and a small decrease in vanadium degree of oxidation occurs [18]. However, using EXAFS it was difficult to prove the presence of V–N bonds in the bulk catalyst structure, because using this technique it was impossible to distinguish N and O ligands in the first coordination shell of vanadium. The only direct technique, which was used by now to identify the presence of V–N bonds in the catalyst, was X-ray photo-electron spectroscopy (XPS). XPS can be used for the analysis of surface species; however, it requires high vacuum conditions, which makes extremely difficult to apply it to *in situ* studies. In the present work we tried to get more information about the reactivity of lattice nitrogen in this catalyst and local environment of vanadium using *in situ* valence-to-core XES at V Kβ fluorescence line. A catalyst with V/Al ratio of 0.25, which was shown in the previous studies to be the most active, was prepared following the synthesis protocol mentioned in the literature [14] with the same reaction conditions (500 °C, O_2:C_3H_8:NH_3 = 3:1.25:1). *In situ* XAS at V K-edge vanadium also measured in the same experiment provided us complimentary information on the local structure and the oxidation state of vanadium in the catalyst. The data obtained by valence-to-core XES and XAS should correspond to the average material composition from 3 to 5 μm layer, which we considered as the bulk structure. The *ex situ* XPS analysis was performed after the catalytic tests in order to confirm the presence and the nature of surface species.

2. Experimental

A V/Al/O catalyst with V/Al molar ratio of 0.25 was prepared according to a published protocol [14]. The catalyst was produced by co-precipitation of solutions containing 0.01 M ammonium metavanadate and 0.01 M aluminum nitrate at 60 °C. Ammonium metavanadate was dissolved in hot water (60 °C) under stirring and then nitric acid (50 wt%) was added until the pH reached 3.0. When the solution of aluminum nitrate was added to the mixture, the latter became red-orange with pH of 2.5. Then the pH was increased up to 5.5 by adding ammonium hydroxide solution (25 wt%) and the mixture was maintained in these conditions for 1 h. The yellow precipitate was washed with ethanol and dried in vacuum at 120 °C.

Valence-to-core XES experiments at V Kβ line were performed at ID26 (X-ray absorption and emission spectroscopy beamline) at ESRF (Grenoble, France). The electron energy of the storage ring was 6.0 GeV; the ring current varied between 150 and 200 mA. The incident energy (5500 eV), which was 35 eV above the V K-edge, was selected by means of a pair of Si(2 2 0) single crystals. Higher harmonics were suppressed by two Si mirrors at 3.0 mrad. The beam size on the sample was 0.3 mm horizontal and 1 mm vertical with a total flux of about 10^{13} photons/s. We used an analyzer that employs the (3 3 3) Bragg plane of one spherically bent (R = 850 mm) Ge wafer, 89 mm in diameter. The energy bandwidth in the X-ray emission detection was 0.6 eV. An avalanche photodiode (APD) was used as the detector. The counting time per XES spectrum was 5 min. The XES spectra were recorded continuously during the whole period of catalytic test. The Kβ main and Kβ satellite lines were measured from 5390 to 5442 eV with 0.5 eV step and normalized by the integral spectral intensity. To perform quantitative analysis of the valence-to-core XES data we fitted the $K\beta_{1,3}$ main line contribution using pseudo-Voigt functions and subtracted it as a background. After each XES spectrum one V K-edge XAS spectrum of the catalyst was measured in a quick scan mode from 5442 to 5742 eV with 0.1 eV step (2 min scan per scan) using Si diode detector, which recorded the total fluorescence yield. The XAS spectra were normalized to the edge jump equal to 1. Analysis of the pre-edge region was conducted after subtracting the edge step contribution. The "pre-edge intensity" was defined to be the maximum intensity in this net pre-edge multiplet. The "pre-edge peak centroid" was defined to be the center of mass of this multiplet. For better understanding the effect of li-

Table 2
List of the consequent treatments of V/Al/O catalyst.

Treatment	Gas atmosphere	Temperature (°C)	Time of exposure (h:min)
A – initial state[a]	Air	25	–
B	O_2:C_3H_8:NH_3 = 3:1.25:1	280	During 5 °C/min ramp
C	O_2:C_3H_8:NH_3 = 3:1.25:1	500	2:00
D	O_2:C_3H_8:NH_3 = 3:1.25:1	500	3:00
E	O_2:C_3H_8:NH_3 = 3:1.25:1	500	3:25
F	O_2:C_3H_8:NH_3 = 3:1.25:1	500	4:22
G	O_2:C_3H_8:NH_3 = 3:1.25:1	500	5:35
H	O_2:C_3H_8:NH_3 = 3:1.25:1	500	9:20
I	O_2:C_3H_8:NH_3 = 3:1.25:1.25	500	1:25
J	NH_3	500	4:50
K	He	50	–

[a] Initial state corresponds to the state after drying at 120 °C.

Table 1
List of reference compounds with corresponding vanadium environment.

Compounds	Formal valence	Bond type	Number of bonds	Symmetry[a]	Bond distance (Å)	Reference
VB	0	V–B	7		2.26 × 4, 2.29 × 2, 2.40	[28]
		V–V	4		2.74 × 4	
VC	4	V–C	6	O_h	2.09	[29]
VN	3	V–N	6	O_h	2.07	[30]
V_2O_3	3	V–O	6	O_h	1.96, 2.06	[31]
V-bearing magnetite	3	V–O	6	O_h	2.0	[32]
Goldmanite	3	V–O	6	O_h	1.99	[33]
$V_{1.2}Al_{0.47}Ca_{2.9}Fe_{0.33}Mg_{0.08}Mn_{0.02}Si_3O_{12}$						
V_2O_4	4	V–O	6	O_h	1.76, 1.86, 1.87, 2.01, 2.03, 2.05	[34]
Cavansite	4	V–O	5	P_y	1.60, 1.98 × 4	[35]
$Ca(VO)(Si_4O_{10})\cdot 4H_2O$						
V_2O_5	5	V–O	5	P_y	1.58, 1.78, 1.89 × 2, 2.02	[36]
Vanadinite	5	V–O	4	T_d	1.70	[37]
$Pb_5(VO_4)_3Cl$						
Palenzonaite	5	V–O	4	T_d	1.72	[38]
$As_{0.24}Ca_{2.3}Mn_2Na_{0.7}O_{12}Si_{0.3}V_{2.46}$						
VF_4	4	V–F	6	O_h	1.70 × 2, 1.92 × 4	[39]

[a] O_h, octahedral; T_d, tetrahedral; and P_y, pyramidal.

gands, valence state, and coordination of vanadium on the fine structure of valence-to-core XES and XAS spectra, we also measured different reference compounds: V_2O_5, vanadinite, cavansite, goldmanite, V-substituted magnetite, VN, VC, VB, and VF_4. These compounds were issued from either mineral collections or commercial compounds. The experimental X-ray absorption near edge spectroscopy (XANES) spectra were also compared with the data obtained on different reference compounds by Wong et al. [20], Giuli et al. [21], and Sutton et al. [22].

Valence-to-core XES spectra were calculated on the basis of a full multiple scattering theory using the FEFF8.4 code [23]. Self-consistency of the potential was performed for a 0.52-nm cluster using the Hedin–Lunqvist exchange potential. The additional imaginary part of the potential equal to 0.6 eV was used to take into account the experimental resolution. The geometry of the cluster was constructed based on the standard X-ray diffraction data (Table 1). Full multiple scattering calculations were performed for a 0.6-nm radius. The spectra corresponding to non-equivalent crystallographic positions were averaged. Calculations for the energies of 2s levels for free atoms were performed on the basis of usual Herman–Skillman procedure [45] with exchange parameter taken according to the Schwarz prescription [24].

The *in situ* experiment was performed in the reactor cell described in [19]. Before the catalytic test, the fresh catalyst (115 mg) was pressed into a 13-mm pellet and fixed in the reactor cell. Four Bronkhorst mass flow controllers were used to produce the reaction mixtures containing C_3H_8, O_2, and NH_3 in He with a total flux of 30 ml/min. The reactivity of the catalyst was controlled using on-line VG ProLab mass-spectrometer (ThermoElectron Corporation). Reaction products could be identified but not quantified and thus selectivities have not been calculated. Table 2 presents the conditions in which the XES and XAS spectra were recorded. To remove water the catalyst was pre-heated in the reactor cell up to 120 °C in 20% O_2 in He (5 °C/min). Then, the stoichiometric catalytic mixture (O_2:C_3H_8:NH_3 = 3:1.25:1) was introduced into the reactor cell and the heating was continued up to 500 (5 °C/min). Under these conditions (500 °C, O_2:C_3H_8:NH_3 = 3:1.25:1), the catalyst stayed on-stream for 9 h and 20 min. Then, the reaction atmosphere was changed to ammonia-rich mixture (O_2:C_3H_8:NH_3 = 3:1.25:1.25) and the spectra were recorded for 1 h and 25 min. After this, oxygen and propane feeds were stopped and the measurements were continued in NH_3 atmosphere for 4 h and 50 min. Finally, the catalyst was cooled to 50 °C in He and the last spectrum was recorded.

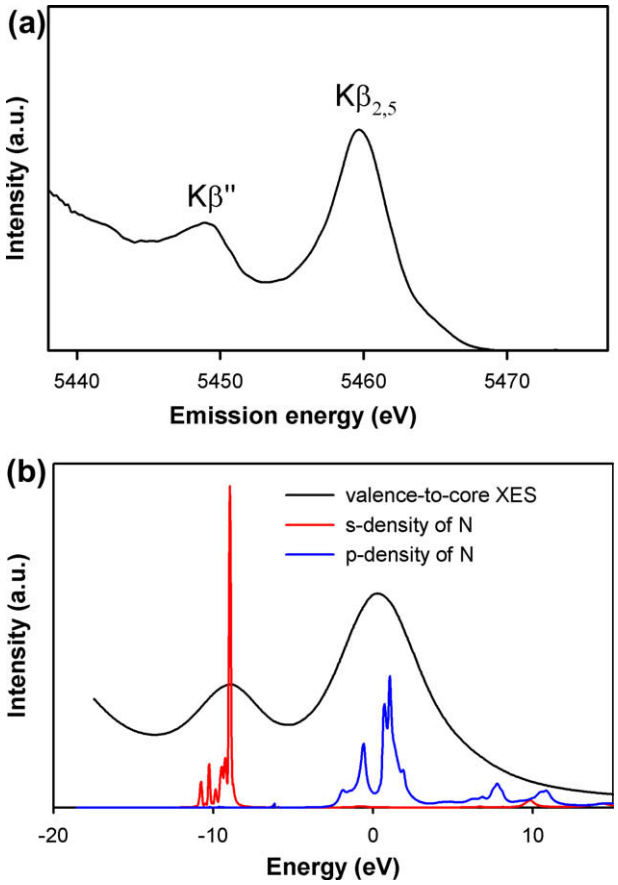

Fig. 1. (a) Experimental valence-to-core XES of VN; (b) full multiple scattering calculations for VN: valence-to-core XES (black line) and partial densities of nitrogen states with s- (red line) and p-symmetry (blue line). (For interpretation of the references to color in this figure legend, the reader is referred to the web version of this article.)

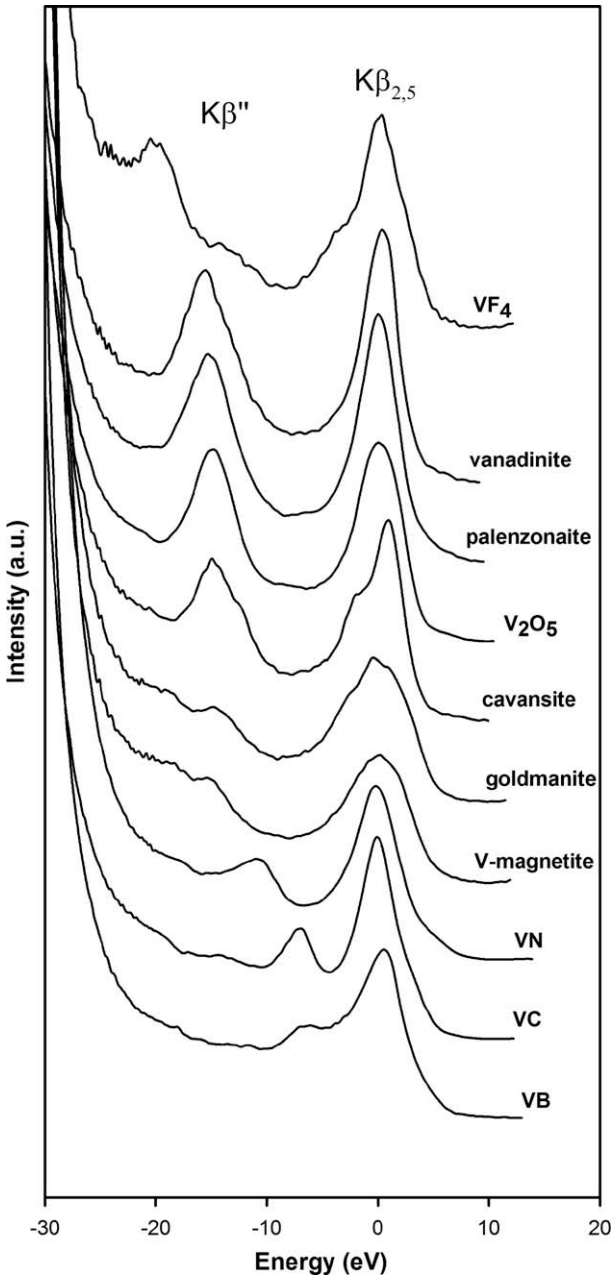

Fig. 2. Experimental valence-to-core XES spectra of the reference compounds.

XPS measurements were performed using a Kratos Axis Ultra DLD spectrometer. The base pressure in the analysis chamber was better than 5×10^{-8} Pa. XPS spectra of N1s, V2p, Al2p O1s, and C1s levels were measured at 90° (normal angle with respect to the plane of the surface) using a monochromated Al Kα X-ray source with a pass energy of 20 eV and a spot size aperture of 300 μm × 700 μm. Charging of the samples was corrected by setting the binding energy of carbon (C1s) at 284.5 eV. The experimental precision of the quantitative analysis, after Shirley background, was considered to be around 10%.

For better comparison we studied the fresh catalyst, the catalyst after *in situ* tests at the synchrotron, and the catalyst after the test in a conventional laboratory apparatus. The conditions of the laboratory test were similar to those used for *in situ* experiment: the catalyst was exposed at 500 °C to the stoichiometric gas mixture (O_2:C_3H_8:NH_3 = 3:1.25:1) for 4 h and cooled to room temperature in He.

3. Results and discussion

3.1. Valence-to-core XES of vanadium reference compounds

The Kβ emission spectra of 3d elements are composed of main lines corresponding to 3p → 1s transitions and satellite lines corresponding to valence-to-core ones [25–27]. Since in chemical compounds valence orbitals of metal interact with ligand orbitals, valence-to-core transitions are structurally and chemically sensitive.

The Kβ satellite lines are situated on the high-energy slope of $K\beta_{1,3}$ main line. The spectrum of the Kβ satellite lines of VN is shown in Fig. 1a. It consists of two main features called $K\beta_{2,5}$ and Kβ″ (or cross-over peak). Full multiple scattering calculations of valence-to-core XES of VN and the corresponding partial densities of ligand (nitrogen) states with s- and p-symmetry are depicted in Fig. 1b. Obviously, the Kβ″ line corresponds to the transitions to the N 2s states, while the $K\beta_{2,5}$ line is due to the band formed of mainly N 2p orbitals. For chemical compounds of 3d metals (Fe, Mn, and Cr) and elements of the second period (B, C, N, O, and F), it was shown [25–27] that the positions of Kβ″ lines relative to the position of $K\beta_{2,5}$ (or Fermi energy) depend almost linearly on the positions of 2s-atomic levels of ligands surrounding metal. To simplify the data analysis we shifted all experimental valence-to-core XES spectra relative to the center of mass of $K\beta_{2,5}$ peak (measured between 5457 and 5459 eV). The spectra of the different reference compounds thus shifted are presented in Fig. 2. The main characteristics of these compounds are gathered in Table 1. One can see that the relative positions of Kβ″ lines of the vanadium ref-

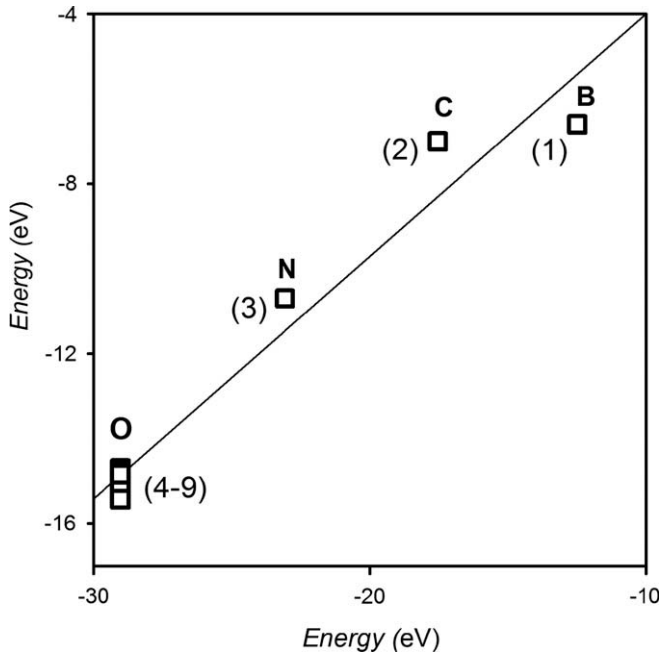

Fig. 3. The correlation between the energies of the 2s-atomic levels of oxygen (O), nitrogen (N), carbon (C), and boron (B) (abscissa) and the positions of the maxima of Kβ" lines (ordinate) for the reference compounds containing these elements in the first coordination shell: (1) VB, (2) VC, (3) VN, (4) V-magnetite, (5) goldmanite, (6) cavansite, (7) V_2O_5, (8) vanadinite, and (9) palenzonaite.

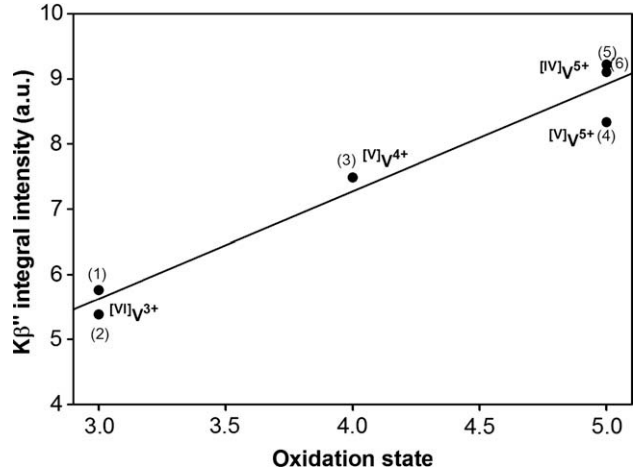

Fig. 4. Correlation of the integral intensity of Kβ″ line and vanadium oxidation state in oxide reference compounds ((1) V-bearing magnetite, (2) goldmanite, (3) cavansite, (4) V_2O_5, (5) palenzonaite, and (6) vanadinite).

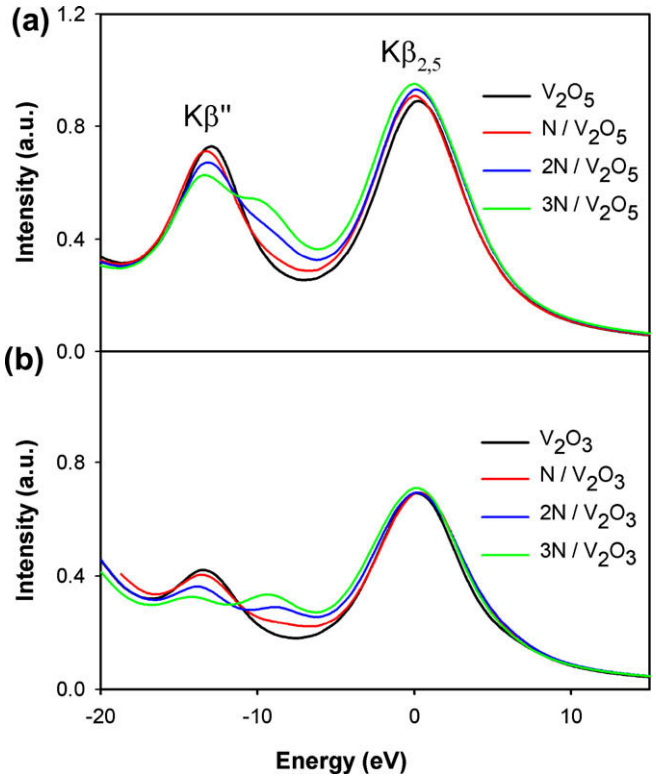

Fig. 5. Full multiple scattering calculations of valence-to-core XES spectra for central vanadium atom in V_2O_5 (a) and V_2O_3 (b) clusters having standard and N-substituted first coordination shell.

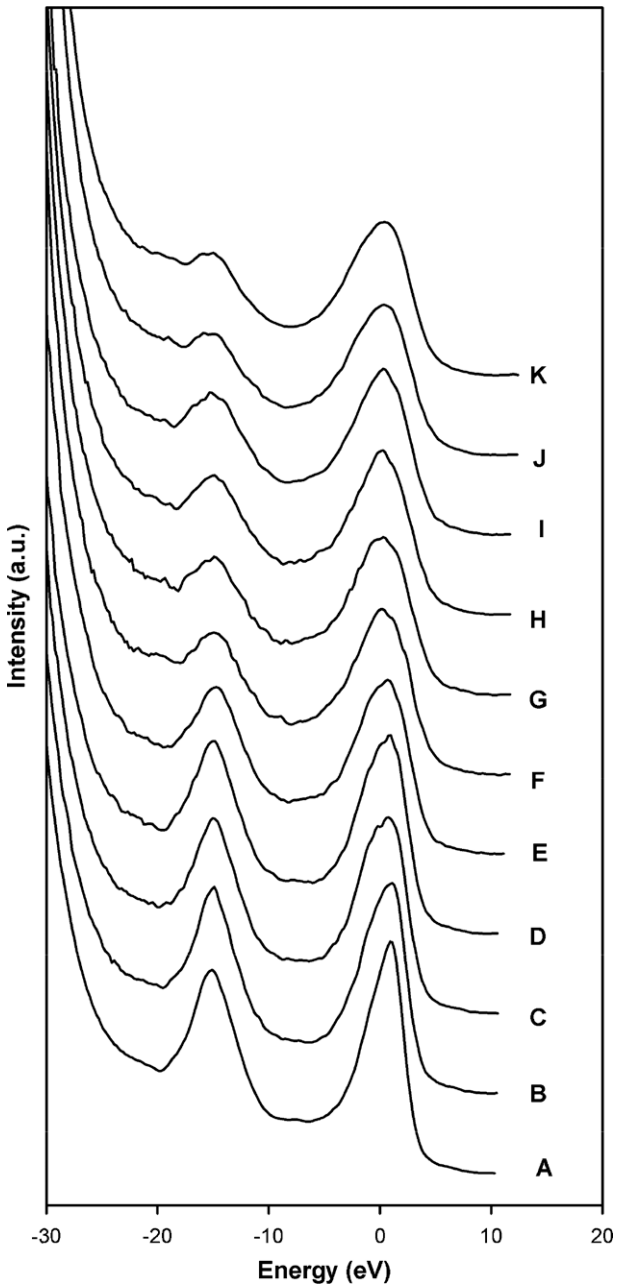

Fig. 6. Valence-to-core XES spectra of vanadium in V/Al/O catalyst under reaction conditions (letters A–J refer to the conditions mentioned in Table 1).

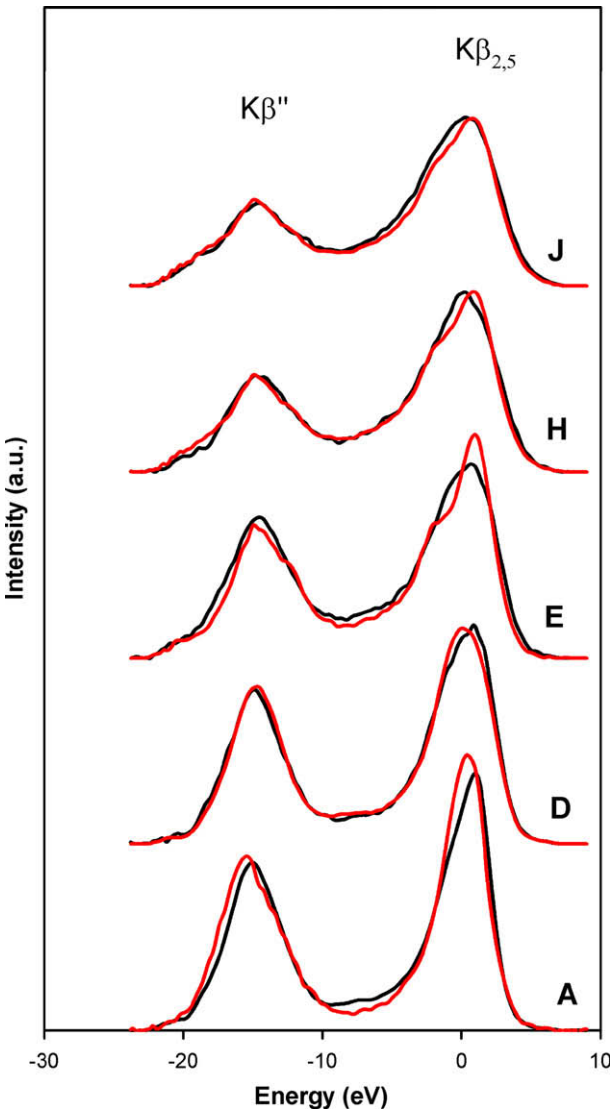

Fig. 7. Valence-to-core XES data (without background) of vanadium in V/Al/O catalyst (black lines, letters A, D, E, H, and J refer to the conditions mentioned in Table 1) in comparison with the spectra of vanadium in different oxide local environment (red lines). A is compared to vanadinite; D is compared to V_2O_5; E is compared to cavansite; H is compared to V-magnetite and cavansite mixture with 4:6 ratio; and J is compared to the linear combination of V-magnetite and cavansite mixture with 6:4 ratio. (For interpretation of the references to color in this figure legend, the reader is referred to the web version of this article.)

erence compounds depend strongly on the nature of the ligands than on the formal oxidation state of vanadium and its local coordination. In Fig. 3, for all reference compounds the positions of maxima of Kβ″ lines are plotted as a function of the energy of 2s-atomic levels of ligands. For oxide reference samples, we have also found the correlations between the intensity of Kβ″ lines and the formal oxidation state of vanadium which are presented in Fig. 4. We will use this correlation later to estimate the vanadium oxidation state in V/Al/O catalyst under working conditions.

Using full multiple scattering calculations we have also tried to estimate the effect of partial substitution of nitrogen for oxygen in the first coordination shell on the shape of valence-to-core XES spectra of vanadium oxides. For this purpose we took 0.6 nm clusters of standard V_2O_3 and V_2O_5 oxides (Table 1) and substituted nitrogen for 1, 2, or 3 oxygen ligands around the central vanadium atom. The results of the full multiple scattering calculations for these clusters are given in Fig. 5 together with the calculated spectra of standard clusters of V_2O_3 and V_2O_5. Substitution of nitrogen for oxygen in the oxide structures led to the appearance of

Table 3
Comparison of the catalytic results obtained in a conventional reactor and in the *in situ* cell for the V/Al/O catalyst [14].

GHSV (L/g/h)	Gas atmosphere	Temp. (°C)	Conv. (%)	$Sel._{ACN}$ (%)	$Rate_{C_3H_8}$ (mol/s/m^2)
16.8	O_2:C_3H_8:NH_3 = 3:1.25:1	500	60	56	14.8×10^{-8}
15.6	O_2:C_3H_8:NH_3 = 3:1.25:1	500	53	–	11.4×10^{-8}

shoulders on the right side of Kβ" lines of oxides, close to the position of Kβ″ line of VN. It seems that the energy positions of Kβ″ lines in vanadium oxides and nitrides do not depend strongly on the formal oxidation state and coordination of vanadium. This result indicates that valence-to-core XES can be used for the analysis of the nature of ligands in the first coordination shell of vanadium even for materials with disordered or unknown local coordination, which is the case of V/Al/O-mixed amorphous oxide catalyst.

3.2. In situ valence-to-core XES of V/Al/O catalyst

Valence-to-core XES spectra obtained during successive *in situ* treatments of V/Al/O catalyst (Table 2) are shown in Fig. 6. In the initial state (spectrum A), the positions and intensities of Kβ″ and $K\beta_{2,5}$ lines indicate that vanadium is fully oxidized. During treatment of the sample in the catalytic mixtures and pure NH_3, the intensity of Kβ″ and $K\beta_{2,5}$ lines progressively decreased. Change in the intensity of Kβ″ and $K\beta_{2,5}$ lines was observed under catalytic mixture at 500 °C (C, D) but were really significant after 3 h and 30 min of exposure of the catalyst in the stoichiometric catalytic mixture (spectra E–F). We detected the first traces of ACN in the gas products using on-line mass-spectrometer already before reaching 500 °C and the conversion of propane reached progressively a steady state and did not change until pure ammonia was introduced into the reactor cell. The catalytic properties obtained in the cell have been compared to those obtained in a conventional reactor in almost similar reaction conditions (Table 3). Certainly because the flux is not flowing through the sample, the conversion rate of propane is slightly lower in the cell. Due to exposure of the catalyst in ammonia (curve J in Fig. 6) the intensities of Kβ″ and $K\beta_{2,5}$ lines further decreased. During cooling of the catalyst in He to 50 °C (curve K in Fig. 6) the XES spectra did not change significantly, which allowed the sample to be used for the XPS analysis.

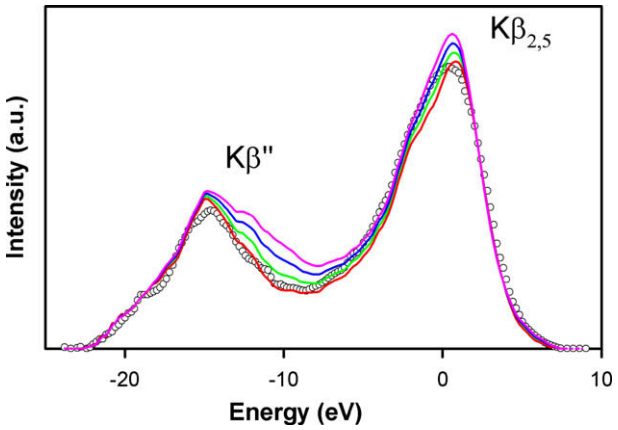

Fig. 8. Valence-to-core XES data (without background) of vanadium in V/Al/O catalyst after exposure in pure NH_3 at 500 °C (white circles) in comparison with the spectra of vanadium in different local environment: red line corresponds to V-magnetite:cavansite ratio of 6:4; green line to V-magnetite:cavansite:VN ratio of 5:4:1 (~2 wt% N); blue line to V-magnetite:cavansite:VN ratio of 4:4:2 (~4 wt% N); and pink line to V-magnetite:cavansite:VN ratio of 3:4:3 (~6 wt% N). (For interpretation of the references to color in this figure legend, the reader is referred to the web version of this article.)

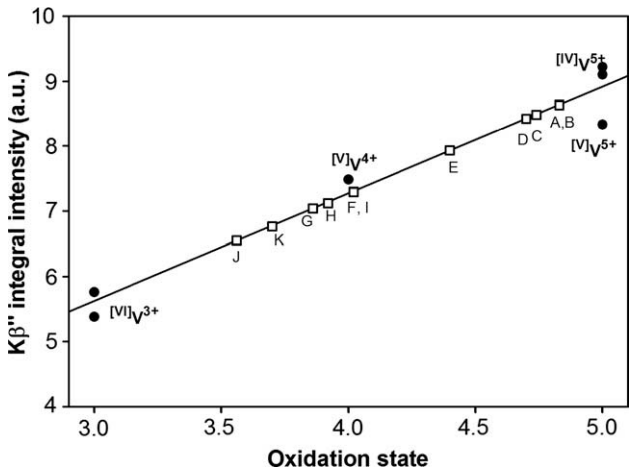

Fig. 9. Estimation of vanadium oxidation state in V/Al/O catalyst after different treatments (letters A–J refer to the conditions mentioned in Table 1) using the integral intensity of Kβ″ lines of oxide reference compounds.

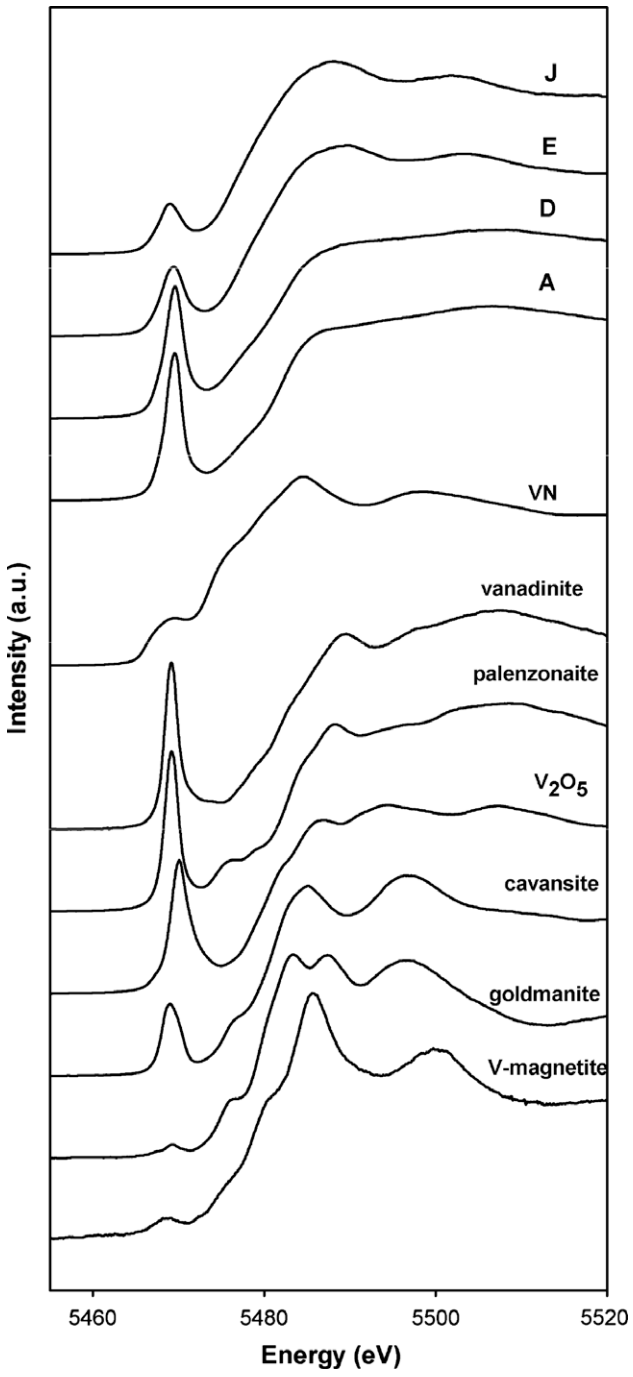

Fig. 10. V K-edge XANES of V/Al/O catalyst under reaction conditions (the letters A, D, E, and J refer to the conditions mentioned in Table 1) and the spectra of the reference compounds.

Table 4
Spectral characteristics of V K-edge XANES of oxide reference compounds and V/Al/O catalyst after different treatments (A–J).

Compound	Formal valence	Number of bonds	Main-edge position (eV)	Pre-edge centroid (eV)	Pre-edge intensity (a.u.)
V-bearing magnetite	3	6	5474.8	5468.1	0.08
Goldmanite	3	6	5474.8	5468.5	0.065
Cavansite	4	5	5481.4	5469.0	0.41
V_2O_5	5	5	5480.6	5470.3	0.76
Palenzonaite	5	4	5483.1	5469.1	0.90
Vanadinite	5	4	5482.4	5469.5	0.97
VN	3	6	5473.4	5468.4	0.14
A			5482.4	5469.4	0.82
B			5482.3	5469.3	0.82
C			5482.3	5469.4	0.74
D			5482.3	5469.3	0.74
E			5476.9	5469.3	0.40
F			5476.9	5469.4	0.38
G			5476.9	5469.4	0.37
H			5476.9	5469.2	0.37
I			5476.9	5469.2	0.35
J			5476.2	5468.8	0.24

Comparison of valence-to-core XES spectra of V/Al/O catalyst with the spectra of the reference compounds shows that during catalytic tests vanadium was progressively reduced. However, we observed neither shift nor splitting of Kβ″ line, which would have indicated bulk nitridation of vanadium atoms. All spectra of V/Al/O catalyst could be fitted as a linear combination of only oxide reference compounds. The results obtained are shown in Fig. 7. Before analysis, $K\beta_{1,3}$ main contributions were subtracted from each spectrum. In the initial state, vanadium is similar to V^{5+} with tetrahedral "VO_4" local coordination (vanadinite and palenzonaite reference compounds). During catalytic process and consequent treatment in ammonia, the spectra transformed and became more similar to the spectra of reduced (V^{4+} and V^{3+}) reference compounds having square pyramidal "VO_5" and octahedral "VO_6" coordination. We also tried to fit the same spectra using VN reference compound. Fig. 8 shows the best fit of the spectrum of V/Al/O catalyst exposed in pure NH_3 *in situ* (J) using the linear combination of the reference compounds including VN. One can see that the best fit corresponds to the composition containing less than 10 mol% of vanadium atoms in nitride local environment, which formally corresponds to ~2 wt% nitrogen in the material.

Since the concentration of nitrogen in the bulk structure of the catalyst is rather small compared to the concentration of oxygen, we used the calibration curve presented in Fig. 4 to estimate the mean oxidation state of vanadium (Fig. 9) at different stages of catalyst treatment. The results confirm that before catalytic testing vanadium in the V/Al/O catalyst was oxidized (formal oxidation state +4.8 ± 0.1). Catalytic reaction and exposure in NH_3 at 500 °C lead to vanadium reduction to the formal oxidation states of +3.8 and +3.5 ± 0.1, respectively.

3.3. In situ XAS

To confirm the results obtained using valence-to-core XES, we also analyzed V K-edge XANES spectra of the V/Al/O catalyst measured under reaction conditions. These spectra are given in Fig. 10 and compared to the spectra of oxide and nitride reference compounds. Table 4 summarizes the spectral characteristics of the main edge and the pre-edge features. It is established that for oxide compounds the positions of the main edge and pre-edge, the pre-edge shape, and intensity depend on the oxidation state and local coordination of vanadium [20–22]. The interplay between the formal valence and the geometry of vanadium in oxide local coordination can be seen in a plot of pre-edge peak intensity vs. pre-edge peak energy found following the approach of Farges et al. [40] for titanium. The same method was already used for the analysis of vanadium local coordination in glasses [21,22]. Fig. 11 shows the data for V/Al/O catalyst after different treatments and for the reference compounds measured in the present work and in previous studies [20–22]. The results confirm that in the initial state vanadium in V/Al/O catalyst oxidized (mainly V^{5+}) and probably has mainly tetrahedral local coordination. Exposure of the

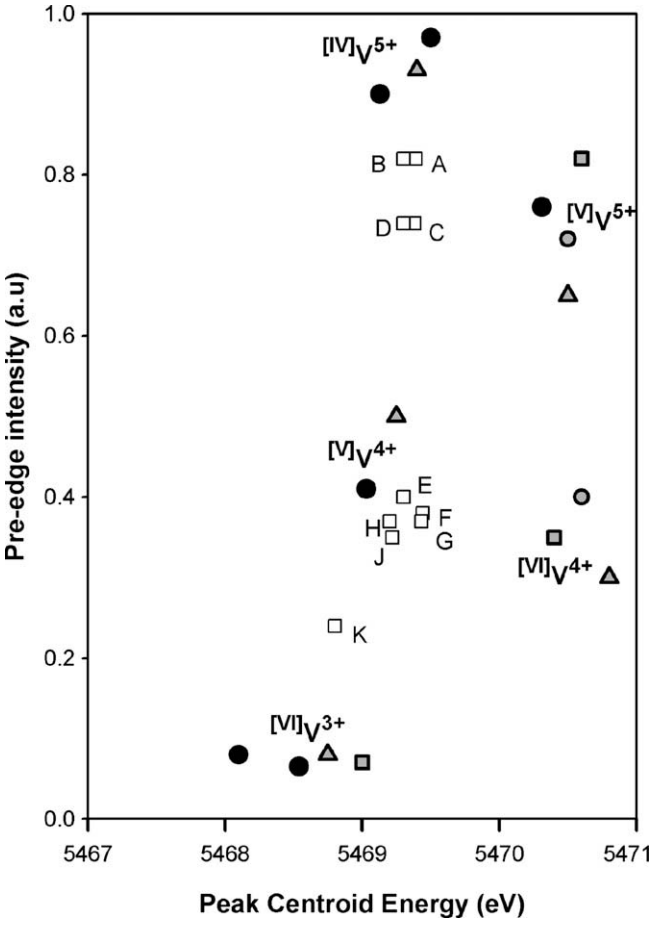

Fig. 11. Pre-edge intensity vs. pre-peak centroid energy for V/Al/O catalyst under different reaction conditions (A–J) (empty squares) in comparison with the reference compounds measured in this work (black circles for V-bearing magnetite, goldmanite, cavansite, V_2O_5, palenzonaite, and vanadinite), by Wong et al. [20] (gray squares for V_2O_3, V_2O_4, and V_2O_5), by Giuli et al. [21] (gray triangles for V-bearing magnetite, V_2O_4, cavansite, V_2O_5, and vanadinite), and Sutton et al. [22] (gray circles for V_2O_4 and V_2O_5).

Table 5
Binding energies and quantitative analysis of V/Al/O samples (before and after catalytic tests) and VN reference compound.

Compound	Line	BE (eV)	State and content (%)	V/Al	N/O	$N^{3-}/(O^{2-}+N^{3-})$
V/Al/O as prepared	V $2p_{3/2}$	517.6	V^{5+} (100%)	0.24	–	–
	Al 2p	74.5				
		530.6	O^{2-} (25%)			
	O 1s	532.2	OH^- (75%)			
V/Al/O after *in situ* test	V $2p_{3/2}$	516.0	V^{4+} (26%)	0.26	0.11	0.06
		517.5	V^{5+} (74%)			
	Al 2p	74.5				
	O 1s	530.6	O^{2-} (80%)			
		532.2	OH^- (20%)			
	N 1s	397.2	N^{3-} (47%)			
		399.0	–NN–[a] (17%)			
		400.9	NH_x (36%)			
V/Al/O after test in standard reactor	V $2p_{3/2}$	516.1	V^{4+} (23%)	0.23	0.04	–
		517.6	V^{5+} (77%)			
	Al 2p	74.5				
	O 1s	530.8	O^{2-} (80%)			
		532.4	OH^- (20%)			
	N 1s	399.2	–NN– (37%)			
		401.2	NH_x (63%)			
VN	V $2p_{3/2}$	514.2	V^{3+} (29%)	–	0.48	0.26
		516.0	V^{4+} (22%)			
		517.5	V^{5+} (49%)			
	O 1s	530.5	O^{2-} (63%)			
		532.4	OH^- (37%)			
	N 1s	396.6				
		397.4	N^{3-} (15%)			
		399.3	N^{3-} (45%)			
		401.3	–NN– (19%)			
			NH_x (21%)			

[a] –NN– refers to M–NN–M species, where M is Al or V.

material in the catalytic mixture followed by NH_3 treatment leads to vanadium reduction to V^{4+}/V^{3+} mixture and the change of the local environment toward mixed square pyramidal and octahedral one.

3.4. XPS analysis

The results of the XPS analysis are summarized in Table 5. The composition of V/Al/O catalyst after its *in situ* treatment and testing in a conventional laboratory apparatus was quite similar. The results were also in good agreement with those of the work by Florea et al. [17]. The surface V/Al atomic ratio was close to the bulk one and did not change after the catalytic treatment. Two values of binding energy were obtained for vanadium before and after the *in situ* experiment at 517.5 and 516.0 eV. These values correspond to the V $2p_{3/2}$ level of V^{5+} and V^{4+}, respectively. In the initial state, the V/Al/O sample contained only V^{5+} on their surface; after the catalytic treatment, V^{5+} was partially reduced to V^{4+}. Two types of oxygen species (O_1 and O_2) were systematically detected in the O 1s spectra (Fig. 12). They have been attributed to lattice oxygen (530.50 eV) and hydroxyl group oxygen (OH^-) (532.20 eV), respectively [41]. The initial catalyst treated only at 120 °C contained mainly OH^- species on the surface; after the catalytic treatment at 500 °C, the concentration of these species strongly decreased. The XPS spectrum of the N 1s region of the catalyst after *in situ* treatment showed three different nitrogen species (Fig. 13) which were attributed to N^{3-} (397.2 eV), di-nitrogeneous species M–NN–M (where M = Al or V) (399.0 eV), and NH_x (400.9 eV) [17,33]. These results were well consistent with those obtained previously by other authors [17] on the same type of compound (similarly prepared, with V/Al = 0.25) after catalytic testing under the same conditions (temperature and gas flow composition) in a conventional testing apparatus. The spectrum of our sample treated in the laboratory apparatus did not show any N^{3-} species, although

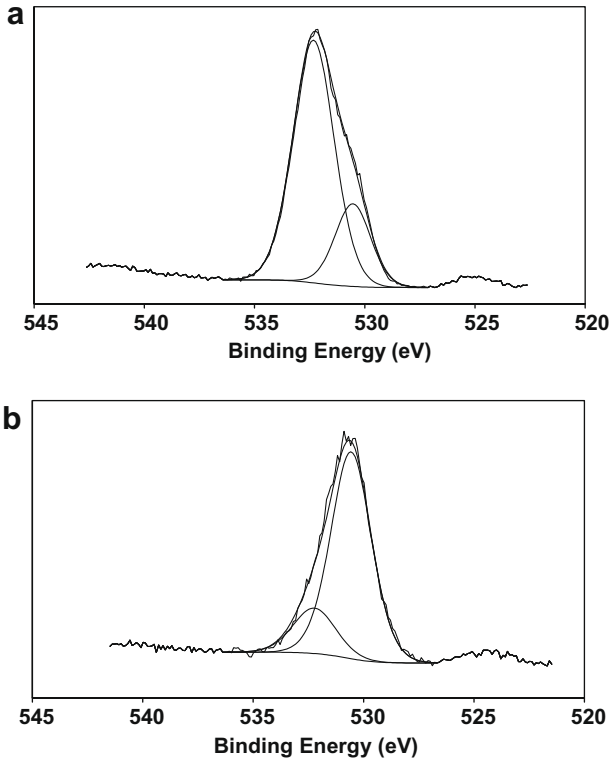

Fig. 12. XPS spectra of the O 1s region of the V/Al/O catalyst before (a) and after *in situ* testing (b).

vanadium was strongly reduced. This can be explained by the fact that the catalyst had been tested for only 4 h. After the *in situ* testing, the N^{3-} content was not very high (6%). However, the real

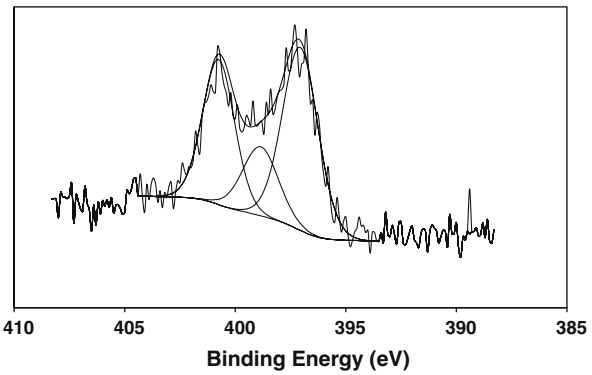

Fig. 13. XPS spectrum of the N 1s region of the V/Al/O catalyst after *in situ* testing (b).

nitrogen content and the concentration of V^{4+} and V^{3+} species on the surface of V/Al/O sample could be underestimated. The analysis of the VN reference compound (Table 4) stored in air showed that the surface of VN contained a significant amount of oxygen and was enriched with oxidized vanadium species (the concentration of V^{5+} was 49%). Similar results have previously been reported showing that after exposure to air, nitrides were unavoidably covered with an oxidized surface layer [42,43]. As for oxide catalysts, it was observed in [44] that the surface of $VSbO_4$ (which had formal oxidation state of +3.7) was also oxidized and contained V^{5+} and V^{4+} species.

4. Conclusions

The results presented in this work demonstrate that combination of valence-to-core XES and XAS can be successfully used for the analysis of vanadium local environment in catalytic materials under reaction conditions. These techniques made it possible to see that vanadium atoms in the bulk of V/Al/O catalyst under the reaction conditions for ACN production (i.e., under the flow of O_2:C_3H_8:NH_3 = 3:1.25:1 mixture at 500 °C) had mixed octahedral or square pyramidal oxygen local environment and contained less than 10% of vanadium atoms in N^{3-} local environment. The oxidation state of vanadium in the catalyst after 9 h on-stream in the catalytic environment followed by treatment in NH_3 at 500 °C was estimated to be 3.8 ± 0.1 and 3.5 ± 0.1, respectively. The fact that vanadium atoms in the bulk of V/Al/O catalyst under reaction conditions were strongly reduced could be the key for catalytic activity. Similar oxidation states of vanadium have already been observed for other efficient propane ammoxidation catalysts such as V/Al/Sb/O and V/Sb/O [2,3,5]. The XPS surface analysis performed *ex situ* after catalytic testing has confirmed the presence of N^{3-}, M–NN–M (with M = Al or V), and NH_x species on the surface. Catalyst on-stream activation seemed to be related to the bulk reduction of vanadium and its nitridation on the surface.

Acknowledgments

Dr. Sigrid Griet Eeckhout (ESRF, Grenoble, France), Dr. Gabriele Giuli (University of Camerino), and Dr. Pieter Glatzel (ESRF, Grenoble, France) are gratefully thanked for having supplied us with the mineral reference samples and for fruitful discussions.

This work has been financed by the French agency, Agence Nationale de la Recherche, Program EFC Environmentally, project AMMOXAN reference ANR-08-EFC-02-01.

References

[1] A.T. Guttmann, R.K. Grasselli, J.F. Brazdil, US Patents 4,746,641 and 4,788,317.
[2] A. Andersson, S.L.T. Andersson, G. Centi, R.K. Grasselli, M. Sanati, F. Trifirò, in: L. Guczi et al. (Eds.), New Frontiers in Catalysis, Elsevier Science, Amsterdam, 1993, p. 691.
[3] G. Centi, S. Perathoner, F. Trifirò, Appl. Catal. A 157 (1997) 143.
[4] S. Albonetti, G. Blanchard, P. Burattin, F. Cavani, S. Masetti, F. Trifiro, Catal. Today 42 (1998) 283.
[5] H. Roussel, B. Mehlomakulu, F. Belhadj, E. Van Steen, J.M.M. Millet, J. Catal. 205 (2002) 97.
[6] T. Ushikubo, K. Oshima, A. Kayou, M. Vaarkamp, M. Hatano, J. Catal. 169 (1997) 394.
[7] M. Hatano, A. Kayo, European Patent 318,295, 1988.
[8] T. Ushikubo, K. Oshima, A. Kayo, T. Umezawa, K. Kiyona, I. Sawaki, European Patent 529,853, 1992.
[9] R.K. Grasselli, D.J. Buttrey, J.D. Burrington, A. Anderssond, J. Holmbergd, W. Ueda, J. Kuboe, C.G. Lugmairf, A.F. Volpe Jr., Top. Catal. 38 (2006) 7.
[10] N. Ballarini, F. Cavani, M. Cimini, F. Trifirò, J.M.M. Millet, U. Cornaroc, R. Catani, J. Catal. 241 (2006) 255.
[11] E. Arcozzi, N. Ballarini, F. Cavani, M. Cimini, C. Lucarelli, F. Trifiro, P. Delichere, J.M.M. Millet, P. Marion, Catal. Today 138 (2008) 97.
[12] B. Deniau, J.M.M. Millet, S. Loridant, N. Christin, J.L. Dubois, J. Catal. 260 (2008) 30.
[13] M. Florea, R. Prada-Silvy, P. Grange, Catal. Lett. 87 (2003) 63.
[14] M. Florea, R. Prada-Silvy, P. Grange, Appl. Catal. A 255 (2003) 289.
[15] M. Olea, M. Florea, I. Sack, R. Prada-Silvy, E.M. Gaigneaux, G.B. Marin, P. Grange, J. Catal. 232 (2005) 152.
[16] N. Blangenois, M. Florea, P. Grange, R. Prada-Silvy, S.P. Chenakin, J.M. Bastin, N. Kruse, B.P. Barbero, L. Cadús, Appl. Catal. A 263 (2004) 163.
[17] M. Florea, R. Prada-Silvy, P. Grange, Appl. Catal. A 286 (2005) 1.
[18] G. Silversmit, H. Poelman, R. De Gryse, W. Bras, S. Nikitenko, M. Florea, P. Grange, S. Delsarte, Catal. Today 118 (2006) 344.
[19] O.V. Safonova, B. Deniau, J.M.M. Millet, J. Phys. Chem. B 110 (2006) 23962.
[20] J. Wong, F.W. Lytle, R.P. Messmer, D.H. Maylotte, Phys. Rev. B 30 (1984) 5596.
[21] G. Giuli, E. Paris, J. Mungall, C. Romano, D. Dingwell, Am. Mineral. 89 (2004) 1640.
[22] S.R. Sutton, J. Karner, J. Papike, J.S. Delaney, C. Shearer, M. Newville, P. Eng, M. Rivers, M.D. Dyar, Geochim. Cosmochim. Acta 69 (2005) 2333.
[23] A.L. Ankudinov, B. Ravel, J.J. Rehr, S.D. Conradson, Phys. Rev. B 58 (1998) 7565.
[24] K. Schwarz, Phys. Rev. B 5 (1972) 2466.
[25] P. Glatzel, U. Bergmann, Coord. Chem. Rev. 249 (1–2) (2005) 65.
[26] V.A. Safonov, L.N. Vykhodtseva, Y.M. Polukarov, O.V. Safonova, G. Smolentsev, M. Sikora, S.G. Eeckhout, P. Glatzel, Phys. Chem. B 110 (2006) 23192.
[27] U. Bergmann, C.R. Horne, T.J. Collins, J.M. Workman, S.P. Cramer, Chem. Phys. Lett. 302 (1999) 119.
[28] O. Schob, E. Parthe, J. Am. Chem. Soc. 74 (1952) 2942.
[29] J. Pflueger, J. Fink, W. Weber, K.P. Bohnen, G. Crecelius, Z. Metal. 54 (1963) 345.
[30] N.S. Gajbhiye, R.S. Ningthoujam, Mater. Res. Bull. 41 (2006) 1612.
[31] R.E. Newnham, Y.M. de Haan, Z. Krist. Kristal. 117 (1962) 235.
[32] M.Z. Stout, P. Bayliss, P. Can. Mineral. 13 (1975) 86.
[33] G.A. Novak, G.V. Gibbs, Am. Mineral. 56 (1971) 791.
[34] A. Andersson, Acta Chem. Scand. 10 (1956) 623.
[35] H.T. Evans Jr., Am. Mineral. 58 (5–6) (1973) 412.
[36] H.G. Bachmann, F.R. Ahmed, W.H. Barnes, Z. Krist. Kristal. 115 (1961) 110.
[37] Y. Dai, J.M. Hughes, Can. Mineral. 27 (1989) 189.
[38] R. Basso, R. Neues Jahrb, Mineral. Monatsh. 3 (1987) 136.
[39] S. Becker, B.G. Mueller, Angew. Chem. 102 (1990) 426.
[40] F. Farges, G.E. Brown Jr., J.J. Rehr, Phys. Rev. B 56 (1997) 1809.
[41] S.J. Liao, D.G. Huang, D.H. Yu, J. Photochem. Photobiol. A 168 (2004) 7.
[42] Z.H. Yang, P.J. Cai, L.Y. Chen, J. Alloys Compd. 420 (2006) 229.
[43] M.Y. Liao, Y. Gotoh, H. Tsuji, J. Ishikawa, J. Vac. Sci. Technol. A22 (2004) 146.
[44] A. Andersson, S.L.T. Andersson, G. Centi, R.K. Grasselli, M. Sanati, F. Trifiro, Appl. Catal. A 113 (1994) 43.
[45] F. Herman, S. Skillman, Atomic Structure Calculation, Prentice-Hall, Englewood Cliffs, NJ, 1963.